Chemistry Europe
European Chemical Societies Publishing

WILEY VCH

Excellence in Chemistry Research

Announcing our new flagship journal

- Gold Open Access
- Publishing charges waived
- Preprints welcome
- Edited by active scientists

Meet the Editors of *ChemistryEurope*

Luisa De Cola
Università degli Studi di Milano Statale, Italy

Ive Hermans
University of Wisconsin-Madison, USA

Ken Tanaka
Tokyo Institute of Technology, Japan

Chemistry–A European Journal
Research Article
doi.org/10.1002/chem.202203493
Chemistry Europe
European Chemical Societies Publishing
www.chemeurj.org

Fast Motions Dominate Dynamics of Intrinsically Disordered Tau Protein at High Temperatures

Anton Abyzov,[d] Eckhard Mandelkow,[e, f] Markus Zweckstetter,[c, d] and Nasrollah Rezaei-Ghaleh*[a, b, c]

Abstract: Reorientational dynamics of intrinsically disordered proteins (IDPs) contain multiple motions often clustered around three motional modes: ultrafast librational motions of amide groups, fast local backbone conformational fluctuations and slow chain segmental motions. This dynamic picture is mainly based on ^{15}N NMR relaxation studies of IDPs at relatively low temperatures where the amide-water proton exchange rates are sufficiently small. Less is known, however, about the dynamics of IDPs at more physiological temperatures. Here, we investigate protein dynamics in a 441-residue long IDP, tau protein, in the temperature range from 0–25 °C, using ^{15}N NMR relaxation rates and spectral density analysis. While at these temperatures relaxation rates are still better described in terms of amide group librational motions, local backbone dynamics and chain segmental motions, the temperature-dependent trend of spectral densities suggests that the timescales of fast backbone conformational fluctuations and slower chain segmental motions might become inseparable at higher temperatures. Our data demonstrate the remarkable dynamic plasticity of this prototypical IDP and highlight the need for dynamic studies of IDPs at multiple temperatures.

Introduction

Proteins exert their functions through motions. In addition to translational and rotational diffusive motions, folded proteins undergo conformational fluctuations around a stable average three-dimensional structure.[1] Various dynamic modes of folded proteins are activated in a hierarchical manner at different temperatures.[2] Unlike folded proteins, intrinsically disordered proteins (IDPs) do not adopt a single three-dimensional structure but populate a highly heterogeneous ensemble of conformers without any persisting average structure.[3] Conformational motions in IDPs often contain numerous modes of distance and reorientational dynamics occurring at a wide range of length and time scales.[4] Because of alterations in the size and shape of protein molecules, conformational dynamics of IDPs are coupled with their rotational diffusion.[5] Due to these complications, protein dynamic studies in IDPs are more challenging than in folded proteins.

Backbone dynamics in IDPs at pico-to-nanosecond timescales have been investigated mainly through ^{15}N NMR relaxation measurements.[6] Various theoretical approaches such as spectral density mapping,[7] extended model-free analysis[8] and continuous distribution of correlation times[9] have been used to interpret NMR relaxation rates of IDPs in terms of protein dynamic parameters. More recently, the combination of high-field NMR relaxation and molecular dynamic (MD) simulation techniques facilitated the dynamic interpretation of NMR relaxation rates in IDPs.[10] In addition, integrating high-field NMR relaxation and microseconds-long MD simulation with low-field proton relaxometry and/or single-molecule nanosecond fluorescence correlation spectroscopy techniques enabled access to reorientational and distance dynamics of IDPs at multiple length and timescales.[11] In particular, the experimental characterization of slow, small-amplitude motions at single-residue resolution has been facilitated by combining low-field relaxation and high-field detection, named high-field relaxometry.[12] Overall, the reorientational dynamics of IDPs appear to be clustered around three main components: an

[a] Dr. N. Rezaei-Ghaleh
Institute of Physical Biology
Heinrich Heine University Düsseldorf
Universitätsstraße 1, D-40225 Düsseldorf (Germany)
E-mail: Nasrollah.Rezaie.Ghaleh@hhu.de
[b] Dr. N. Rezaei-Ghaleh
Institute of Biological Information Processing,
IBI-7: Structural Biochemistry
Forschungszentrum Jülich,
D-52428 Jülich (Germany)
[c] Prof. M. Zweckstetter, Dr. N. Rezaei-Ghaleh
Department of NMR-based Structural Biology
Max Planck Institute for Multidisciplinary Sciences
Am Fassberg 11, D-37077 Göttingen (Germany)
[d] Dr. A. Abyzov, Prof. M. Zweckstetter
Translational Structural Biology Group
German Center for Neurodegenerative Diseases (DZNE)
Von-Siebold-Str. 3a, D-37075 Göttingen (Germany)
[e] Prof. E. Mandelkow
German Center for Neurodegenerative Diseases (DZNE)
Venusberg-Campus 1, D-53127, Bonn (Germany)
[f] Prof. E. Mandelkow
Research Center CAESAR
Ludwig-Erhard-Allee 2, D-53175, Bonn (Germany)

Supporting information for this article is available on the WWW under https://doi.org/10.1002/chem.202203493

ultrafast librational motion of amide groups at tens of picoseconds timescale, fast fluctuations in backbone dihedral angles at hundreds of picoseconds to a few nanoseconds, and slow segmental motions at several to a few tens of nanoseconds.[8d,10c] Besides, studies of the temperature dependence of NMR relaxation rates have provided insights into the activation energies associated with different motional modes in IDPs.[8d,10d]

A technical challenge in ^{15}N NMR relaxation studies of IDPs is the high rate of amide-water proton exchange rate in IDPs, which compromises the sensitivity of NMR experiments at physiological temperatures and pHs.[13] Due to this limitation, the NMR relaxation studies of IDPs are often conducted at low temperatures and/or acidic pH where the amide-water proton exchange rates are sufficiently slow.

It is therefore unclear how well the above-mentioned picture can describe dynamics in IDPs at physiological conditions. Here, we take a prototypical IDP, tau protein, and investigate its temperature-dependent backbone dynamics using spectral density analysis of ^{15}N NMR relaxation rates. The range of measurement temperatures is 0–25 °C, still below physiological temperature and below the temperatures of 27 or 30 °C used in dynamical studies of IDPs in refs. [8b,c], however temperature-dependent investigation of tau protein dynamics enables us to observe a trend and extrapolate it to higher temperatures. Tau protein is a 441 residue-long IDP, with an amino acid composition enriched in positive, negative and hydrophilic residues. It has a domain structure composed of an acidic N-terminal domain, a proline-rich middle region, five relatively basic pseudo-repeats and an almost neutral C-terminal region (Figure 1A). Tau is a microtubule-associated protein predominantly located in the axons of mature neurons, and its missorting into the somatodendritic compartment of neurons, hyperphosphorylation and oligomeric and fibrillar aggregation are involved in neurodegeneration-related tauopathies.[14] Our NMR results demonstrate that the chain backbone dynamics (excluding N–H group librations) in the tau protein might be better described with only one component at high temperatures, where the contribution of segmental motions to ^{15}N relaxation decreases and the timescales of segmental motional modes that still contribute approach the timescale of local chain motions.

Results and Discussion

First, the ^{15}N,^{1}H correlation spectrum of tau protein was measured at 5 °C, where a narrow dispersion of amide proton chemical shifts typical of IDPs was observed (Figure 1B). Next, the ^{15}N,^{1}H correlation spectra were measured at a temperature range 0–25 °C at 5 °C steps. Due to fast amide-water proton exchange rates at higher temperatures and their adverse effects on NMR signal intensities, no NMR experiment at temperatures above 25 °C was recorded. The temperature-dependent peak displacements enabled transferring peak assignments already known at 5 °C to other temperatures (Figure 1C).[15] Knowing the ^{15}N,^{1}H correlation peak assignments at different temperatures, it was possible to study the temperature-dependence of backbone dynamics in tau protein through ^{15}N NMR relaxation experiments.

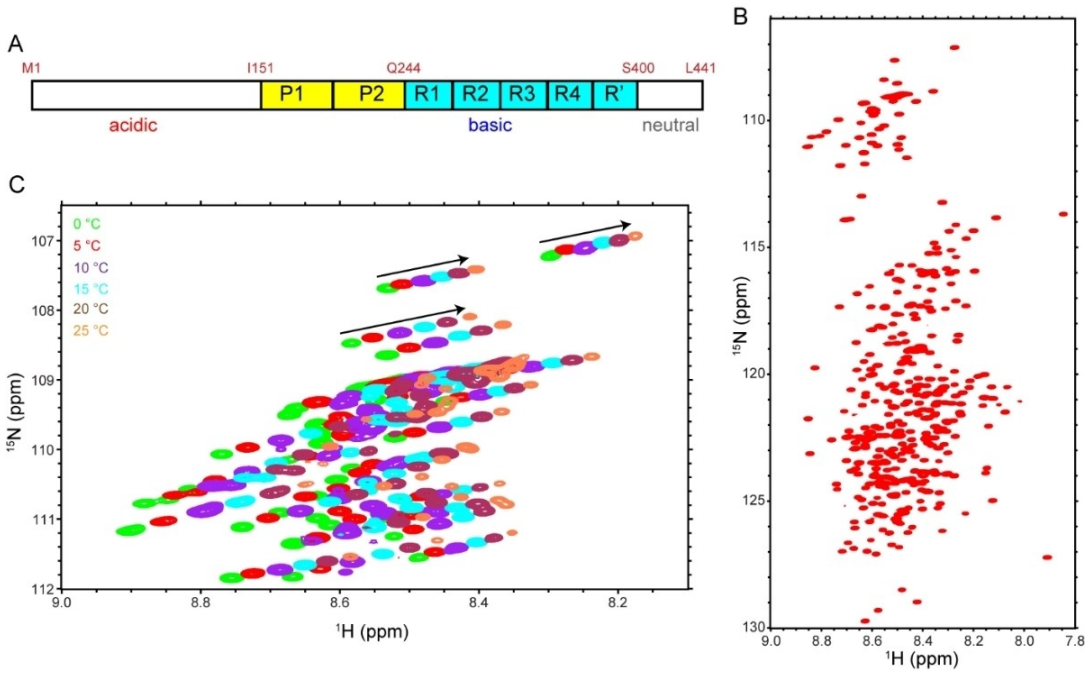

Figure 1. A) Sequence domains of the 441-residue long tau protein, highlighting its proline-rich (P1 and P2) and repeat (R1–R4 and R') domains. B) The ^{15}N,^{1}H HSQC spectrum of tau protein, measured at 5 °C. Note the narrow dispersion of amide proton chemical shifts, a typical characteristic of IDPs. C) Superposition of a selected region containing glycine cross peaks from ^{15}N,^{1}H HSQC spectra of tau protein recorded at 0, 5, 10, 15, 20 and 25 °C. The gradual temperature-induced peak displacements (highlighted by arrows) were used to transfer peak assignments already known at 5 °C to higher temperatures.

Figure 2A shows the ^{15}N longitudinal spin-lattice (R_1) relaxation rates of tau protein at different temperatures. The ^{15}N R_1 rates are predominantly determined by the spectral density term $J(\omega_N)$, representing reorientational motions of corresponding N–H groups at frequency ω_N. In line with the relatively poor sensitivity of $J(\omega_N)$ to reorientational dynamics of N–H groups, only little variation in R_1 was observed along the tau sequence. The average R_1 rates were 1.46 ± 0.07, 1.45 ± 0.07, 1.44 ± 0.09 and 1.37 ± 0.10 s^{-1}, respectively at 0, 5, 15 and 25 °C, displaying only slight temperature-dependent decrease of R_1 in particular between 15 and 25 °C.

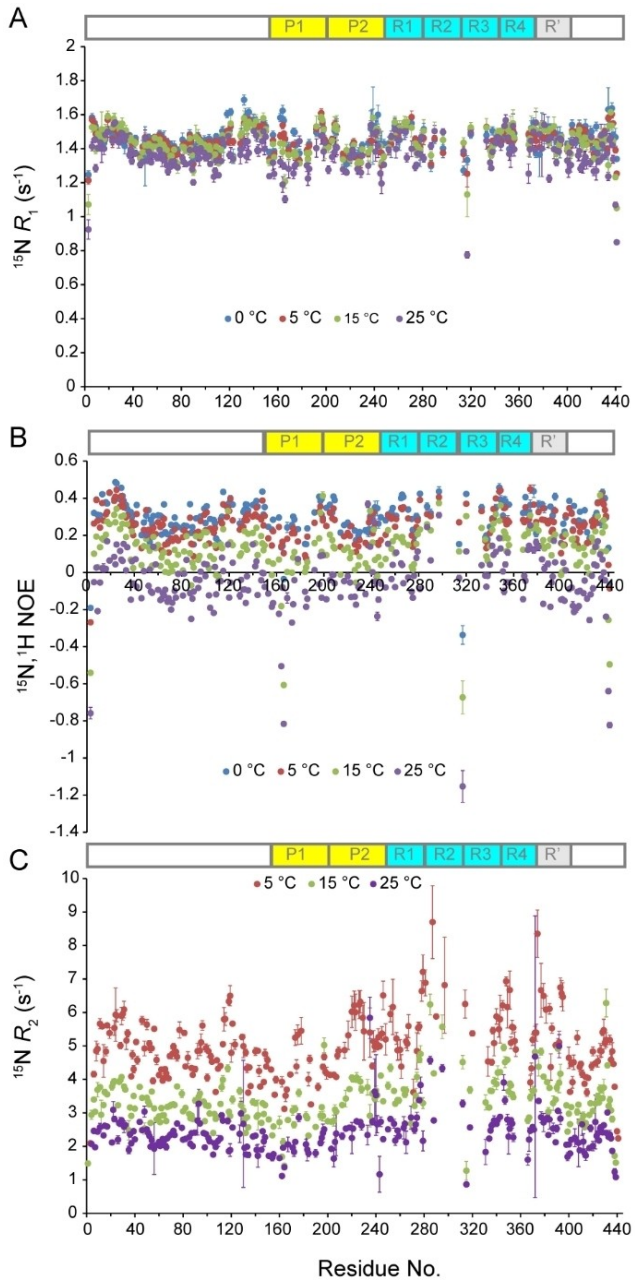

Figure 2. Temperature-dependence of ^{15}N NMR relaxation rates in tau protein. A) ^{15}N longitudinal spin-lattice (R_1) relaxation rates of tau protein, measured at 0, 5, 15 and 25 °C, shown along the sequence of tau. B) Residue-specific ^{15}N,^{1}H nuclear Overhauser enhancement (NOE) values of tau protein measured at 0, 5, 15 and 25 °C. A temperature-dependent decrease in NOE values reflects larger picoseconds dynamics of N–H groups at higher temperatures. C) ^{15}N transverse spin-spin (R_2) relaxation rates of tau protein, measured at 5, 15 and 25 °C. An overall temperature-dependent decrease in ^{15}N R_2 rates is observed. The domain diagram of tau protein is shown at the top of each panel.

Figure 2B shows the ^{15}N,^{1}H NOE of tau protein at the studied temperatures of 0–25 °C. The dynamic-dependence of ^{15}N,^{1}H NOEs is governed by the ratio $J(<\omega_H>)/J(\omega_N)$, which is particularly sensitive to motions of N–H groups at picosecond timescales. The average NOEs were 0.29 ± 0.10, 0.26 ± 0.09, 0.13 ± 0.14 and −0.05 ± 0.17, respectively at 0, 5, 15 and 25 °C. In general, the small values of ^{15}N,^{1}H NOEs indicate large picoseconds dynamics in tau protein in accordance with its intrinsically disordered character. In addition, the temperature-dependent decrease in NOEs reflects the larger picoseconds dynamics of tau protein at higher temperatures.

Unlike ^{15}N R_1 rates and ^{15}N,^{1}H NOEs, the ^{15}N transverse spin-spin (R_2) relaxation rates are predominantly determined by the spectral density function at frequency 0, J(0), which in IDPs is particularly sensitive to slow segmental motions occurring at the timescale of residue-specific rotational correlation times (τ_c or τ_{slow}) of around several to a few tens of nanoseconds. To determine the ^{15}N R_2 rates, we followed two approaches: the $R_{1\varrho}$-based and *CCR* (η_{xy})-based R_2 measurements (Supporting Figures S1–S2, see Methods for details). The R_2 rates obtained from these two approaches were in close agreement: the slope of fitted *CCR*-based R_2 vs. $R_{1\varrho}$-based R_2 line was 0.99 ± 0.01, with R^2 of 0.93 (Supporting Figure S3). Here, we report the *CCR*-based R_2 rates, which are in principle devoid of conformational exchange contributions to R_2 and therefore better represent the intrinsic dynamics of the studied protein. Figure 2C shows the ^{15}N R_2 rates measured at 5, 15 and 25 °C resulting in average ^{15}N R_2 rates of 4.99 ± 0.99, 3.36 ± 0.69 and 2.41 ± 0.59 s^{-1}, respectively. The temperature-dependent decrease in ^{15}N R_2 rates reflects a decrease in τ_c values connected to slow motions of tau protein and/or a decrease in the relative amplitude of such slow motions compared to faster sub-τ_c motions. These slow motions are most likely segmental motions of tau protein, because the global motion of 441-residue long intrinsically disordered tau protein is too slow to significantly contribute to rotational autocorrelation function (ACF) of N–H groups and affect ^{15}N relaxation rates.[16]

Based on the ^{15}N R_1 rates and ^{15}N,^{1}H NOEs measured at different temperatures, the spectral density terms $J(\omega_N)$ and $J(<\omega_H>)$ can be derived in dependence of temperature. As pointed out above, the $J(\omega_N)$ does not exhibit a high sensitivity to the temperature-dependent dynamics. Conversely, the $J(<\omega_H>)$ showed significant increase by temperature, indicating larger picoseconds dynamics at higher temperatures (Figure 3A).

As shown previously, the temperature dependence of $J(<\omega_H>)$ is determined by the energy barrier against predominantly librational motions of N–H groups and local backbone motions, instead of solvent viscosity.[8d] Accordingly, the temperature dependence of the $J(<\omega_H>)$ of tau protein was significantly smaller than the temperature dependence of viscosity (Figure 3A). The spectral density analysis of ^{15}N R_1 and R_2 rates and ^{15}N,^{1}H NOEs allows determining J(0) in addition to

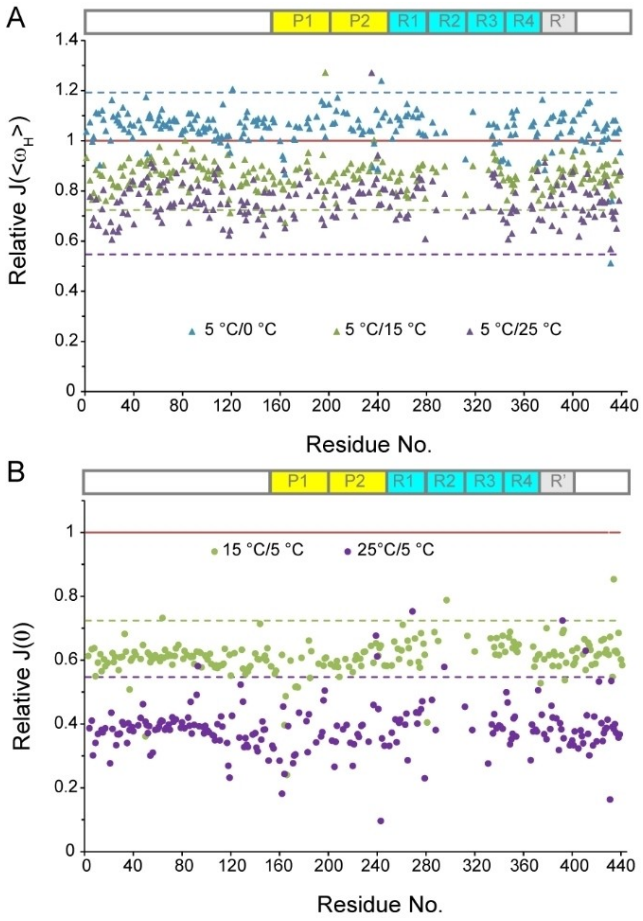

Figure 3. Spectral density analysis of ^{15}N NMR relaxation rates of tau protein, in dependence of temperature. A) The spectral density at average proton frequency, $J(<\omega_H>)$ shows a temperature-dependent increase, which is smaller than the relative change in temperature/viscosity (T/η) ratio (dashed lines). B) The spectral density at 0 frequency, J(0), shows a temperature-dependent decrease, which exceeds the relative change in T/η ratio (dashed lines). The T/η ratio (relative to 5 °C, shown as dashed lines) represents a reference level in which spectral densities would be determined exclusively according to temperature-dependence of T/η ratio. The $J(<\omega_H>)$ and J(0) values are normalized relative to their values at 5 °C, either directly (in B, as J(0) is directly proportional to rotational correlation times, hence supposedly to T/η ratio), or inversely (in A, as $J(<\omega_H>)$ is inversely proportional to rotational correlation times hence supposedly to T/η ratio). The domain diagram of tau is shown at the top of panels A and B.

$J(\omega_N)$ and $J(<\omega_H>)$. The J(0) is sensitive to slow motions at the timescale of τ_c, which in IDPs are predominantly contributed by viscosity-dependent segmental motions.[8d,10c] As shown in Figure 3B, the J(0) values of tau protein were decreasing with temperature, indicating shorter τ_c and/or smaller relative contributions of segmental motions at higher temperatures. Notably, the temperature dependence of J(0) values exceeded the temperature dependence of viscosity, consistent with a significant decrease in the relative amplitude of segmental motions at higher temperatures (Figure 3B).

The J(ω) vs. J(0) relations provide additional information on dynamics in IDPs, especially in regards with whether their relaxation-contributing dynamics are dominated by motions on single or multiple timescales.[7b,c,17] At 5 °C, the $J(\omega_N)$ or $J(<\omega_H>)$ vs. J(0) relations in tau protein showed a clear deviation from the simple theoretical relations describing motions of the protein chain and N–H groups with only one or two Lorentzian components (Figure 4A, B). This suggests the presence of more than one component in the relaxation-active motions of the tau protein chain. Upon increasing the temperature to 15 and 25 °C, an overall decrease in $J(\omega_N)$ and particularly J(0) and an increase in $J(<\omega_H>)$ were observed. The description of protein backbone dynamics at 15 and 25 °C still deviates from the single- or two-component curves, however, if the trend is maintained at temperatures above 25 °C (black arrows in Figure 4), the J(ω) and $J(<\omega_H>)$ vs. J(0) relations would be pushed towards the theoretical relation describing motions of protein chain and N–H groups with only one or two Lorentzian components (red and blue curves in Figure 4, respectively).

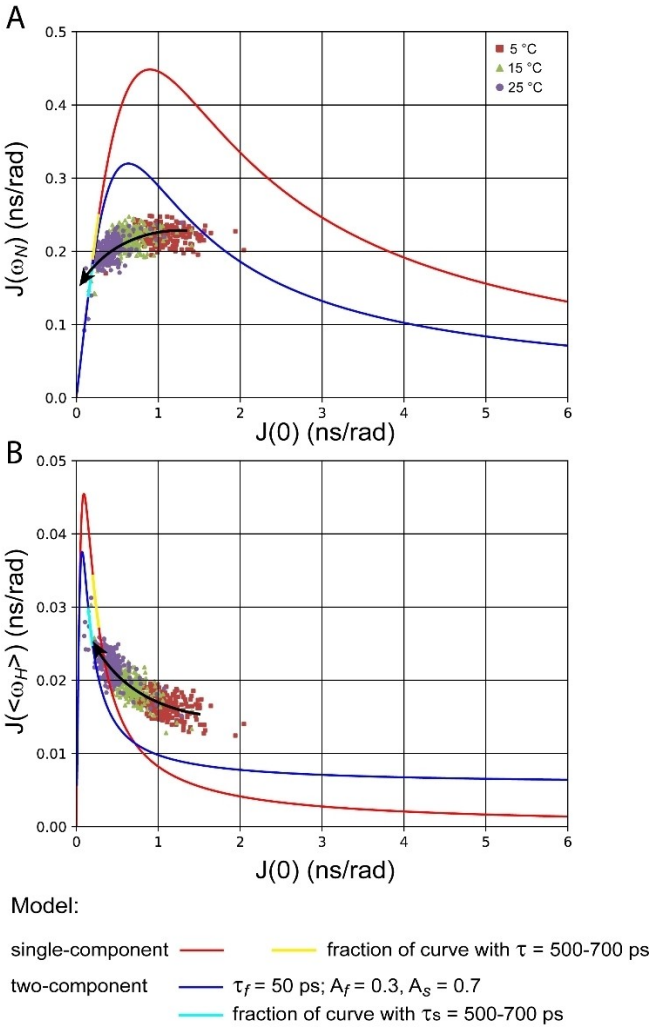

Figure 4. Spectral density analysis of ^{15}N NMR relaxation rates of tau protein, in dependence of temperature. The $J(\omega_N)$ vs. J(0) (A) and $J(<\omega_H>)$ vs. J(0) (B) relations at 5 (red squares), 15 (green triangles) and 25 °C (purple circles) show a clear deviation from the theoretical relation expected for a single or two-Lorentzian motion (solid red and blue curves). However, the general trend (black arrows) suggests that with a temperature rising above 25 °C, the $J(\omega_N)$ or $J(<\omega_H>)$ vs. J(0) relations might be pushed towards the theoretical single or two-Lorentzian curves (red or blue lines, correspondingly). See text for further details.

The single- and two-component dynamics are difficult to distinguish in the converged region. Detailed inspection of the curve describing a single-component motion, though, reveal that the described trend approaches the spectral density values of the single-component motion at quite different correlation times on $J(\omega_N)$ vs. J(0) and $J(<\omega_H>)$ vs. J(0) relation plots. These plots, however, represent the same parametric curve in three dimensions (J(0), $J(\omega_N)$ and $J(<\omega_H>)$) with τ as parameter, where J(0) values increase uniformly with τ. Whereas on the $J(\omega_N)$ vs. J(0) plot the timescale of 500 ps seems to be quite slow for the trend (bottom end of the yellow section on Figure 4A), on the $J(<\omega_H>)$ vs. J(0) plot the timescale of 700 ps is quite fast (bottom end of the yellow section on Figure 4B). Therefore, unless the described trend on the $J(<\omega_H>)$ vs. J(0) plot makes a significant jump towards higher $J(<\omega_H>)$ values with temperature, the spectral density values at higher temperature would be better fit to a two-component model which, in addition to chain motions (with timescales of about 500–700 ps, light blue sections in Figure 4), has another component for N–H group librations (the example corresponding to a timescale of 50 ps and a contribution of 30% for N–H librational motions, typical values reported in previous studies of IDPs, for example in,[8d] is shown in Figure 4). Indeed, a single-component description of protein dynamics would imply here amide group librations on timescales of hundreds of picoseconds, which is significantly slower than tens of picoseconds reported for unfolded and intrinsically disordered proteins and domains by other groups.[8d,18] A three-component description of protein dynamics would fit into the converged region only if the contribution of segmental motions is very small and/or their timescale is close to the timescale of local backbone motions, transforming it to an effectively two-component model (Supporting Figure S4).

NMR-based dynamics studies of several IDPs have converged to a picture in which the multiscale reorientational dynamics of IDPs can be reasonably approximated by three modes of motions: librational motions, local conformational dynamics involving backbone dihedral angle fluctuations, and segmental motions.[8d,10a,c,d,11–12] At low temperatures, the characteristic correlation times of these three motional modes are sufficiently separated from each other, therefore it is reasonable to assume the effective mutual independence of these motions and therefore decompose the rotational ACF of each N–H group of the protein into its three independent components, as required in the (extended) model-free analysis of ^{15}N NMR relaxation rates.[19] Upon increasing temperature, the timescales of librational motions and conformational fluctuations are altered according to their specific activation energy barriers, whereas the temperature-dependence of the timescale of segmental motions is governed mainly by the change in the $\eta(T)/T$ ratio where $\eta(T)$ is the temperature-dependent viscosity.[8d] As the activation energy of local chain motions was suggested to be lower than the $\eta(T)/T$ ratio describing temperature dependence of chain segmental motions,[8d] the timescale of the latter would decrease faster with temperature than the timescale of the former; therefore, at a sufficiently high temperature their timescales would theoretically become identical. However, based on timescales and activation energies described in another IDP system,[8d] where this temperature would be calculated at above the water boiling point, we do not believe that the true matching of timescales could happen at physiological temperatures. Rather, at some sufficiently high temperature these timescales approach each other so closely that they would become inseparable, as the adiabatic approximation would not be valid anymore.[8d] Our data suggests that the effective merging of motions and timescale inseparability could occur at temperatures much closer to physiological temperature.

In addition to the timescales, the relative amplitude of these three modes of motions may be altered by temperature. In particular, the temperature-induced enhancement in local motions may force the rotational ACFs of N–H groups to decay to zero before the segmental motions at longer timescales could provide any further contribution to their decay.[8d] Previous studies have shown that the N–H motions of IDPs at temperatures as high as 298–303 K can still be better described by a three-component than single-component dynamics.[8b–d,12] Our results are consistent with these reports but the temperature-dependent trend of spectral densities show that the increase in temperature pushes the multi-component description of reorientational dynamics of tau protein at low temperatures towards a description with a reduced set of dynamic components at high temperatures. An explanation for this behaviour might be that the timescales of various components become more difficult to separate from each other at higher temperatures, while at the same time the contribution from segmental motions decreases with temperature. It is also notable that a recent single-molecule fluorescence anisotropy-based study of tau protein has revealed the presence of two families of tau conformers with distinct local and segmental rotational dynamics.[20] It is therefore expected that temperature dependence of tau dynamics is considerably influenced by potential population shifts as a function of temperature. Whether the observed temperature-dependent trend of tau dynamics in this study is protein-specific or instead a generic feature of IDPs remains to be investigated in future, however, considering the large size of tau protein and the diverse physicochemical properties of its domains, it is reasonable to suggest its dynamical trend as a generic feature of IDPs.

The amide groups of IDPs are exposed to the surrounding solvent and severely prone to rapid amide-water proton exchange rates at physiological temperature.[13] Consequently, the ^{15}N NMR relaxation-based studies of protein dynamics in IDPs are often performed at temperatures significantly lower than the physiological temperature. Our NMR results demonstrate the remarkable dynamic plasticity of IDPs in response to temperature and highlights the importance of investigating IDPs' dynamics at multiple temperatures. Notably, the reduced sensitivity of ^{15}N relaxation to slower segmental motions may be overcome by engineering short stable helices into IDP chains to reduce amplitudes of fast internal motions.[8d] This approach may be useful at higher temperatures to compensate for the potential inseparability between fastest segmental motions with fast internal motions.

Dynamic studies of IDPs at higher temperatures may be made possible through a shift to acidic pH where amide-water exchange is effectively quenched, or preferably, through switching to non-exchangeable nuclear spins such as ^{13}C. In this regard, we note that the newly developed singlet-filtered NMR experiments allow the study of the relaxation of non-exchangeable Hα protons of glycines in IDPs.[21] In addition, the singlet relaxation times of glycines provide novel sensitive probes of motions in IDPs applicable at high temperatures.[22]

Conclusion

Our study of the temperature dependence of the internal dynamics in the intrinsically disordered protein tau shows that its multi-component, relaxation-active dynamics at low temperature might become an effectively two-component dynamics with increasing temperature, as the timescale of chain segmental motions progressively approaches that of local backbone motions and its contribution decreases as local motions gain in amplitude. The results thus reveal enhanced plasticity of an IDP in response to increasing temperature and highlight the importance of studying IDP dynamics at multiple temperatures.

Experimental Section

NMR spectroscopy: NMR experiments were conducted at a 701.25 MHz proton Larmor frequency spectrometer equipped with a room-temperature probe. The NMR sample contained ~0.3 mM uniformly ^{15}N-labeled human tau protein (residue 1-441; 2N4R tau) in 60 mM sodium phosphate buffer (pH 6.0, with 42 mM NaCl) in 90%/10% v/v H_2O/D_2O.

^{15}N,^{1}H correlation peak assignments were made through ^{15}N,^{1}H HSQC experiments at 0, 5, 10, 15, 20 and 25 °C and the transfer of peak assignments already known at 5 °C.[15] ^{15}N relaxation experiments were performed at 0, 5, 15 and 25 °C. The steady-state ^{15}N–^{1}H heteronuclear Overhauser enhancements (NOE) were measured with a proton saturation block of 5 s and total recycle delay of 8 s. A train of 120° proton pulses was used during the saturation block. The ^{15}N longitudinal relaxation rates ($\mathbf{R}_1$) were measured using conventional pulse sequence schemes with relaxation delays of 10, 60, 150, 250, 400, 600 and 1000 ms.[23] The ^{15}N transverse relaxation rates ($\mathbf{R}_2$) were measured through two ways: (i) ^{15}N longitudinal relaxation rates in the rotating frame ($\mathbf{R}_{1\rho}$) were measured with relaxation delays of 20, 40, 60, 100, 160 and 240 ms and ^{15}N spin-lock field strength of 2.0 kHz as described in,[24] with ^{15}N carrier frequency set in the middle (118 ppm) of the ^{15}N resonance dispersion in tau protein. In heteronuclear NOE and $R_{1\varrho}$ measurements the PEP ("preservation of equivalent pathways") scheme was used to improve the sensitivity of NMR experiments. The ^{15}N transverse relaxation rates ($\mathbf{R}_2$) were then derived from the relation: $R_2 = \frac{(R_{1\rho} - R_1 . cos^2\theta)}{sin^2\theta}$, where $\theta \equiv \tan^{-1}(\frac{\nu_1}{\Omega})$, ν_1 is the ^{15}N spin-lock field strength (in Hz) and Ω is the resonance offset from the spin-lock carrier (Hz), and (ii) transverse cross-correlated relaxation (*CCR*, η_{xy}) rates between ^{1}H,^{15}N dipole-dipole and ^{15}N chemical shift anisotrpy (CSA) relaxation mechanisms were measured using relaxation delays of 50, 75, 100 and 125 ms.[25] The *CCR* rates were then converted to R_2 rates through Equation (1):

$$R_2 = \kappa\, \eta_{xy} + 1.3\, \sigma \tag{1}$$

where

$$\sigma = (NOE - 1) \times R_1 \times \frac{\gamma_N}{\gamma_H} \tag{2}$$

is the ^{15}N,^{1}H cross-relaxation rate and γ_H and γ_N are the gyromagnetic ratios of ^{1}H and ^{15}N nuclei. The κ value is a constant value of 1.3466, calculated from the theoretical equations of ^{15}N relaxation rates, based on the ^{15}N CSA of −170 ppm and the angle between the symmetry axis of ^{15}N CSA tensor and the N–H vector of 22°.[26] All NMR relaxation rate measurements were performed in the FID-interleaved manner and the heat correction and compensation elements were introduced in the beginning of recycle delays.

NMR spectra were processed with NMRPipe,[27] and the peak intensities were obtained by Sparky 3 (T. D. Goddard and D. G. Kneller, SPARKY 3, University of California, San Francisco). Using an in-house Mathematica script, the $\mathbf{R}_1$ and $\mathbf{R}_{1\rho}$ rates were obtained through fitting intensity data to mono-exponential decay functions. The errors in R_1 and $R_{1\varrho}$ were obtained through 500 Monte-Carlo simulations of relaxation data. The errors in R_2 were estimated through propagation of errors in R_1 and $R_{1\varrho}$. NOE values were calculated as the ratio of the peak intensities between saturated and reference spectra, with errors estimated from the noise values in these spectra. *CCR* rates were calculated through fitting, as described in,[25] with uncertainties represented by the standard error of fitting parameters.

Reduced spectral density mapping of the ^{15}N R_1 and R_2 rates and ^{15}N–^{1}H cross-relaxation rates (σ) to spectral densities at zero, ^{15}N and effective ^{1}H frequency (J(0), $J(\omega_N)$ and $J(<\omega_H>)$, respectively) was performed using the following Equation (3)–(5):

$$J(<\omega_H>) = {}^{\sigma}/_{5d} \tag{3}$$

$$J(\omega_N) = \frac{1}{3d + c}\ (R_1 - 1.4\sigma) \tag{4}$$

$$J(0) = \frac{1.5}{3d + c}\ (R_2 - \frac{R_1}{2} - 0.6\sigma) \tag{5}$$

where

$$d = \frac{1}{4}\left(\frac{\mu_0}{4\pi}\right)^2 \left(\frac{(\hbar\gamma_H\gamma_N)^2}{r_{N-H}^6}\right) \tag{6}$$

and

$$c = \frac{(\omega_N \Delta\sigma)^2}{3} \tag{7}$$

in which the physical constants had their usual meanings, and the H–N bond length (r_{N-H}) of 1.02 Angstrom and the ^{15}N CSA magnitude (Δσ) of −170 ppm were used.[7a] Uncertainties in spectral density values were estimated through error propagation. The theoretical $J(\omega_N)$ vs. J(0) relation for a single-component motion was calculated according to the following equation:

$$J(\omega_N) = \frac{J(0)}{1 + 6.25\ \omega_N^2\ J(0)^2} \tag{8}$$

Acknowledgements

N. R.-G. acknowledges the Deutsche Forschungsgemeinschaft (German Research Foundation, DFG) for research grants RE 3655/2-1 and 3655/2-3. M. Z. was supported by the European Research Council (ERC) under the EU Horizon 2020 research and innovation programme (grant agreement No. 787679). We thank Yunior Cabrales Fontela for help in initial analysis of NMR data. Open Access funding enabled and organized by Projekt DEAL.

Conflict of Interest

The authors declare no conflict of interest.

Data Availability Statement

The data that support the findings of this study are available from the corresponding author upon reasonable request.

Keywords: intrinsically disordered protein · NMR relaxation · protein dynamics · spectral density analysis · tau protein

[1] K. Henzler-Wildman, D. Kern, *Nature* **2007**, *450*, 964–972.
[2] J. R. Lewandowski, M. E. Halse, M. Blackledge, L. Emsley, *Science* **2015**, *348*, 578–581.
[3] a) N. Rezaei-Ghaleh, M. Blackledge, M. Zweckstetter, *ChemBioChem* **2012**, *13*, 930–950; b) M. R. Jensen, M. Zweckstetter, J. R. Huang, M. Blackledge, *Chem. Rev.* **2014**, *114*, 6632–6660.
[4] B. Schuler, A. Soranno, H. Hofmann, D. Nettels, *Annu. Rev. Biophys.* **2016**, *45*, 207–231.
[5] V. Wong, D. A. Case, A. Szabo, *Proc. Natl. Acad. Sci. USA* **2009**, *106*, 11016–11021.
[6] C. Charlier, S. F. Cousin, F. Ferrage, *Chem. Soc. Rev.* **2016**, *45*, 2410–2422.
[7] a) N. A. Farrow, O. W. Zhang, A. Szabo, D. A. Torchia, L. E. Kay, *J. Biomol. NMR* **1995**, *6*, 153–162; b) J. F. Lefevre, K. T. Dayie, J. W. Peng, G. Wagner, *Biochemistry* **1996**, *35*, 2674–2686; c) P. Kaderavek, V. Zapletal, A. Rabatinova, L. Krasny, V. Sklenar, L. Zidek, *J. Biomol. NMR* **2014**, *58*, 193–207.
[8] a) M. Buck, H. Schwalbe, C. M. Dobson, *J. Mol. Biol.* **1996**, *257*, 669–683; b) S. N. Khan, C. Charlier, R. Augustyniak, N. Salvi, V. Dejean, G. Bodenhausen, O. Lequin, P. Pelupessy, F. Ferrage, *Biophys. J.* **2015**, *109*, 988–999; c) M. L. Gill, R. A. Byrd, A. G. Palmer, *Phys. Chem. Chem. Phys.* **2016**, *18*, 5839–5849; d) A. Abyzov, N. Salvi, R. Schneider, D. Maurin, R. W. H. Ruigrok, M. R. Jensen, M. Blackledge, *J. Am. Chem. Soc.* **2016**, *138*, 6240–6251; e) W. Adamski, N. Salvi, D. Maurin, J. Magnat, S. Milles, M. R. Jensen, A. Abyzov, C. J. Moreau, M. Blackledge, *J. Am. Chem. Soc.* **2019**, *141*, 17817–17829.
[9] a) A. V. Buevich, J. Baum, *J. Am. Chem. Soc.* **1999**, *121*, 8671–8672; b) K. Modig, F. M. Poulsen, *J. Biomol. NMR* **2008**, *42*, 163–177; c) A. Hsu, F. Ferrage, A. G. Palmer, *Biophys. J.* **2018**, *115*, 2301–2309.
[10] a) N. Salvi, A. Abyzov, M. Blackledge, *J. Phys. Chem. Lett.* **2016**, *7*, 2483–2489; b) O. Stenstrom, C. Champion, M. Lehner, G. Bouvignies, S. Riniker, F. Ferrage, *Curr. Opin. Struct. Biol.* **2022**, *77*, 102459; c) N. Salvi, A. Abyzov, M. Blackledge, *Angew. Chem. Int. Ed. Engl.* **2017**, *56*, 14020–14024; d) N. Salvi, A. Abyzov, M. Blackledge, *Sci. Adv.* **2019**, *5*, eaax2348.
[11] a) N. Rezaei-Ghaleh, G. Parigi, A. Soranno, A. Holla, S. Becker, B. Schuler, C. Luchinat, M. Zweckstetter, *Angew. Chem. Int. Ed. Engl.* **2018**, *57*, 15262–15266; b) N. Rezaei-Ghaleh, G. Parigi, M. Zweckstetter, *J. Phys. Chem. Lett.* **2019**, *10*, 3369–3375.
[12] N. Salvi, V. Zapletal, Z. Jasenakova, M. Zachrdla, P. Padrta, S. Narasimhan, T. Marquardsen, J. M. Tyburn, L. Zidek, M. Blackledge, F. Ferrage, P. Kaderavek, *Biophys. J.* **2022**, *121*, 3785–3794.
[13] a) D. Kurzbach, E. Canet, A. G. Flamm, A. Jhajharia, E. M. Weber, R. Konrat, G. Bodenhausen, *Angew. Chem. Int. Ed. Engl.* **2017**, *56*, 389–392; b) A. F. Faustino, G. M. Barbosa, M. Silva, M. Castanho, A. T. Da Poian, E. J. Cabrita, N. C. Santos, F. C. L. Almeida, I. C. Martins, *Sci. Rep.* **2019**, *9*, 1647.
[14] E. M. Mandelkow, E. Mandelkow, *Cold Spring Harb. Perspect. Med.* **2012**, *2*, a006247.
[15] M. D. Mukrasch, S. Bibow, J. Korukottu, S. Jeganathan, J. Biernat, C. Griesinger, E. Mandelkow, M. Zweckstetter, *PLoS Biol.* **2009**, *7*, e34.
[16] G. Parigi, N. Rezaei-Ghaleh, A. Giachetti, S. Becker, C. Fernandez, M. Blackledge, C. Griesinger, M. Zweckstetter, C. Luchinat, *J. Am. Chem. Soc.* **2014**, *136*, 16201–16209.
[17] S. Morin, *Prog. Nucl. Magn. Reson. Spectrosc.* **2011**, *59*, 245–262.
[18] a) Y. Xue, N. R. Skrynnikov, *J. Am. Chem. Soc.* **2011**, *133*, 14614–14628; b) M. K. Frank, G. M. Clore, A. M. Gronenborn, *Protein Sci.* **1995**, *4*, 2605–2615; c) B. Brutscher, R. Bruschweiler, R. R. Ernst, *Biochemistry* **1997**, *36*, 13043–13053; d) M. L. Gill, R. A. Byrd, A. G. Palmer, III, *Phys. Chem. Chem. Phys.* **2016**, *18*, 5839–5849.
[19] a) G. M. Clore, A. Szabo, A. Bax, L. E. Kay, P. C. Driscoll, A. M. Gronenborn, *J. Am. Chem. Soc.* **1990**, *112*, 4989–4991; b) B. Halle, *J. Chem. Phys.* **2009**, *131*, 224507.
[20] A. K. Foote, L. H. Manger, M. R. Holden, M. Margittai, R. H. Goldsmith, *Phys. Chem. Chem. Phys.* **2019**, *21*, 1863–1871.
[21] S. Mamone, N. Rezaei-Ghaleh, F. Opazo, C. Griesinger, S. Gloggler, *Sci. Adv.* **2020**, *6*, eaaz1955.
[22] S. Mamone, S. Gloggler, S. Becker, N. Rezaei-Ghaleh, *ChemPhysChem* **2021**, *22*, 2158–2163.
[23] A. G. Palmer, 3rd, *Annu. Rev. Biophys. Biomol. Struct.* **2001**, *30*, 129–155.
[24] D. M. Korzhnev, N. R. Skrynnikov, O. Millet, D. A. Torchia, L. E. Kay, *J. Am. Chem. Soc.* **2002**, *124*, 10743–10753.
[25] N. Tjandra, A. Szabo, A. Bax, *J. Am. Chem. Soc.* **1996**, *118*, 6986–6991.
[26] a) J. R. Brender, D. M. Taylor, A. Ramamoorthy, *J. Am. Chem. Soc.* **2001**, *123*, 914–922; b) L. S. Yao, A. Grishaev, G. Cornilescu, A. Bax, *J. Am. Chem. Soc.* **2010**, *132*, 4295–4309.
[27] F. Delaglio, S. Grzesiek, G. W. Vuister, G. Zhu, J. Pfeifer, A. Bax, *J. Biomol. NMR* **1995**, *6*, 277–293.

Manuscript received: November 9, 2022
Accepted manuscript online: December 29, 2022
Version of record online: February 17, 2023